

Scattering of Rydberg excitons by phonon-plasmon modes

Heinrich Stolz^{1,*}  and Dirk Semkat² 

¹ Institut für Physik, Universität Rostock, Albert-Einstein-Str. 24, 18059 Rostock, Germany

² Institut für Physik, Ernst-Moritz-Arndt-Universität Greifswald, Felix-Hausdorff-Str. 6, 17489 Greifswald, Germany

E-mail: heinrich.stolz@uni-rostock.de

Received 27 April 2021, revised 6 July 2021

Accepted for publication 21 July 2021

Published 12 August 2021



Abstract

We propose a new scattering mechanism of Rydberg excitons, i.e., those with high principal quantum numbers, namely scattering by coupled LO phonon-plasmon modes, which becomes possible due to small differences in energies of the states due to different quantum defects. Already in very low-density electron–hole plasmas these provide a substantial contribution to the excitonic linewidth. This effect should allow determining plasma densities by a simple line shape analysis. Whenever one expects that low-density electron–hole plasma is present the plasmon induced broadening is of high significance and must be taken into account in the interpretation.

Keywords: Rydberg excitons, electron–hole plasma, scattering processes, coupled phonon-plasmon modes

(Some figures may appear in colour only in the online journal)

1. Introduction

The experimental observation of excitons with high quantum numbers up to $n = 25$ in cuprous oxide Cu_2O at low temperatures [1] has triggered a series of studies on the behavior of these Rydberg excitons in electric and magnetic fields, as maser materials, for studies of quantum properties of matter etc (for an overview see [2]). On the other hand we expect that Rydberg excitons are strongly influenced by the presence of electron–hole plasma. Indeed, it has been found that the presence of plasma with densities around 10^{10} cm^{-3} already quenches the absorption of P states with high quantum numbers and leads to an additional broadening of the exciton states [3]. Recently, we discussed the interactions of Rydberg excitons with a low-density electron–hole plasma within a many-particle theory [4, 5] to understand the observations. While the quenching of the lines can be explained straightforwardly by


the Mott effect [4, 6], caused mainly by the shift of the band gap with increasing plasma density, using perturbation theory we found almost no change in the imaginary part of the exciton self-energy [5].

However, what is not considered in such an approach is the interaction between different exciton states mediated by the plasma excitations themselves, i.e., the exciton-plasmon interaction. This is expected to be strong if the plasmons themselves are coupled to polar optical phonons, as is usual the case in a polar semiconductor [7, 8]. In this contribution we show that in case of Rydberg excitons with very small binding energies, which are furthermore split because of additional interactions due to the non-parabolicity of the band structure and other central cell effects [9–12], the exciton scattering by LO-plasmons can be quite strong leading to a substantial increase in excitonic linewidth already at very low plasma densities of the order of 10^{11} cm^{-3} that should be easily detectable experimentally.

2. General considerations: exciton states and overlap integrals

Quite generally, the linewidth $\hbar\Gamma_i$ of a state i is given by Fermi's golden rule as

* Author to whom any correspondence should be addressed.

 Original content from this work may be used under the terms of the [Creative Commons Attribution 4.0 licence](https://creativecommons.org/licenses/by/4.0/). Any further distribution of this work must maintain attribution to the author(s) and the title of the work, journal citation and DOI.

$$\Gamma_i = \frac{2\pi}{\hbar} \sum_f |M(i \rightarrow f)|^2 \delta(E_i - E_f). \quad (1)$$

Here f denotes the possible final states of all scattering processes characterized by the transition matrix element M of the interaction under consideration. We consider scattering processes of excitons due to plasmons of an electron–hole plasma. The general expression for the matrix elements of a two-band Wannier exciton, where electron and hole scatter independently, has the form [13]

$$\begin{aligned} M(\vec{K}, nlm, \vec{K}', n'l'm', \vec{Q}, \sigma) \\ = \left[\Xi_{c,v}^{\sigma}(\vec{K} - \vec{K}') W(nlm, n'l'm', \alpha_h \vec{Q}) \right. \\ \left. - \Xi_{v,c}^{\sigma}(\vec{K} - \vec{K}') W(nlm, n'l'm', -\alpha_e \vec{Q}) \right] \delta(\vec{K} - \vec{K}' \mp \vec{Q}), \end{aligned} \quad (2)$$

with the upper sign for Stokes, the lower sign for Antistokes scattering. The overlap functions W are given as

$$W(nlm, n'l'm', \vec{q}) = \int d\vec{r} \phi_{nlm}(\vec{r})^* \phi_{n'l'm'}(\vec{r}) \exp(i\vec{q} \cdot \vec{r}), \quad (3)$$

with $\phi_{nlm}(\vec{r})$ denoting the exciton wave functions with quantum numbers n, l, m and

$$\alpha_e = m_c^*/M, \quad \alpha_h = m_h^*/M, \quad M = m_c^* + m_h^*. \quad (4)$$

$\Xi_{c,v}^{\sigma}(\vec{K} - \vec{K}')$ denote the strengths of the electron and hole plasmon-interactions including the occupations number of the plasmons given by the usual Bose distribution function $n_B(\omega, T) = 1 / (\exp(\hbar\omega/k_B T) - 1)$.

Since we are interested in the scattering of optical excited p -excitons, we have $l = 1$ and $m = 0, \pm 1$. However, due to the non-spherical interaction between electrons and holes in Cu_2O (see e.g. [11, 12]), the actual exciton states are a complicated mixture of envelope functions and Bloch states of valence and conduction bands. Since plasmons and LO phonons cannot flip the spin of an electron and a hole, scattering can only occur between the same spin states. These can be denoted as one para and three ortho states

$$\begin{aligned} P &= \frac{1}{\sqrt{2}}(\uparrow_v \downarrow_c - \downarrow_v \uparrow_c) \\ O_{yz} &= \frac{i}{\sqrt{2}}(\uparrow_v \uparrow_c - \downarrow_v \downarrow_c) \\ O_{xz} &= \frac{1}{\sqrt{2}}(\uparrow_v \uparrow_c + \downarrow_v \downarrow_c) \\ O_{xy} &= -\frac{i}{\sqrt{2}}(\downarrow_v \uparrow_c + \uparrow_v \downarrow_c). \end{aligned} \quad (5)$$

So we have to expand all states involved in the scattering process into their ortho and para components.

Each state is uniquely determined by the representation of the symmetry group, except for the case of an accidental degeneracy. For all group theoretical calculations we used the tables from [14]. Here the initial states of the scattering

are the optically excited states with a P envelope, which are given by

$$\begin{aligned} \Gamma_4^- \otimes (\Gamma_7^+ \otimes \Gamma_6^+) &= (\Gamma_7^- \oplus \Gamma_8^-) \otimes \Gamma_6^+ \\ &= (\Gamma_2^- \oplus \Gamma_5^-) \oplus (\Gamma_3^- \oplus \Gamma_4^- \oplus \Gamma_5^-), \end{aligned} \quad (6)$$

from which only the Γ_4^- state interacts with light. Expressed in their ortho and para contributions, these states look like

$$\begin{aligned} |P8, X\Gamma_4^-\rangle &= -\frac{1}{\sqrt{2}}P_y O_{xy} - \frac{1}{\sqrt{2}}P_z O_{xz} \\ |P8, Y\Gamma_4^-\rangle &= -\frac{1}{\sqrt{2}}P_x O_{xy} - \frac{1}{\sqrt{2}}P_z O_{yz} \\ |P8, Z\Gamma_4^-\rangle &= -\frac{1}{\sqrt{2}}P_x O_{xz} - \frac{1}{\sqrt{2}}P_y O_{yz}. \end{aligned} \quad (7)$$

To characterize a state uniquely we will give the envelope (cubic) symmetry of the state, the representation of envelope and hole spin and the representation and basis function itself.

Defining the coordinate system so that the light propagates along the z axis, which would be quite natural, we excite by light polarized along the x direction the state $|P8, X\Gamma_4^-\rangle$. From this state we can scatter into all states with O_{xy} and O_{xz} spin character. As we have for the states with an S envelope

$$\begin{aligned} |S, \Gamma_2^+\rangle &= SP \\ |S, XY\Gamma_5^+\rangle &= SO_{xy} \\ |S, XZ\Gamma_5^+\rangle &= SO_{xz} \\ |S, YZ\Gamma_5^+\rangle &= SO_{yz}, \end{aligned} \quad (8)$$

we can scatter into the $|S, XY\Gamma_5^+\rangle$ and $|S, XZ\Gamma_5^+\rangle$ states. In the same way we can treat the other P states and the D states. The list of all these states can be found in appendix A. States with higher angular momentum need not to be considered, as their overlap functions (3) are smaller by at least two orders of magnitude.

For the D states we have the following decomposition

$$\begin{aligned} (D \otimes \Gamma_7^+) \otimes \Gamma_6^+ &= (\Gamma_3^+ + \Gamma_5^+) \otimes \Gamma_7^+ \otimes \Gamma_6^+ \\ &= \Gamma_3^+ \otimes \Gamma_7^+ \otimes \Gamma_6^+ + \Gamma_5^+ \otimes \Gamma_7^+ \otimes \Gamma_6^+ \\ &= (\Gamma_8^+ \otimes \Gamma_6^+) + (\Gamma_6^+ \otimes \Gamma_6^+ + \Gamma_8^+ \otimes \Gamma_6^+) \\ &= (\Gamma_3^+ + \Gamma_4^+ + \Gamma_5^+) \\ &\quad + (\Gamma_1^+ + \Gamma_4^+ + \Gamma_3^+ + \Gamma_4^+ + \Gamma_5^+). \end{aligned} \quad (9)$$

The first bracket denotes the states derived from the Γ_3^+ D states, which are also nominated as $D3$ states, while the states in the second bracket are designated as $D5$ using the decomposition of the representations of the full rotation group into those of the cubic group. So $|D5, 8, 5XY\rangle$ denotes the state in the Γ_5^+ representation transforming like xy and derived from the D envelopes with Γ_5^+ symmetry and envelope-hole symmetry Γ_8^+ .

Checking table A1, we see that the $|P8, X\Gamma_4^- \rangle$ excitons can scatter into all these states, except the pure Γ_3^+ para states. Using these relations, we can reduce the overlap integrals over the exciton states into a sum over overlap integrals of hydrogen-like angular momentum states, thereby neglecting a possible change of the wave functions due to non-spherical interactions [12].

As the scattering processes have to fulfill both conservation of energy and quasi-momentum, the exact energetic positions of the different states are important. Recently, quite a lot of papers have been published that investigated this fine structure both from the experimental [9–11] and the theoretical point of view [11, 12]. Designating the energy difference of the $|P8, X\Gamma_4^- \rangle$ state and the S and D states by ΔE_{PX} the dependence on principal quantum number can be described in form of a quantum defect [9–11]

$$\Delta E_{XP}(n) = \frac{\delta_{XP}}{n^\beta}, \quad (10)$$

with constants δ_{XP} . From the experimentally determined energy differences [11, 15] we get $\delta_{55P} = -32$ meV, $\beta = 3$; $\delta_{PD385} = 35$ meV, $\beta = 2.75$; $\delta_{PD584} = 25$ meV, $\beta = 3$. All other states are almost degenerate [12] and will be designated as A with $\delta_{PDA} = 16$ meV, $\beta = 3$.

We expand the plane wave in (3) into spherical harmonics

$$\begin{aligned} \exp(i\vec{Q} \cdot \vec{r}) &= 4\pi \sum_{l=0}^{\infty} \sum_{m'=-l}^l i^l j_l(Qr) \\ &\times Y_{lm'}^*(\vartheta_Q, \varphi_Q) Y_{lm'}(\vartheta, \varphi). \end{aligned} \quad (11)$$

We can write the overlap function for scattering from a hydrogen-like P state into any other hydrogen-like angular momentum state as

$$\begin{aligned} W(n1m, n' L m', \vec{Q}) &= i^{(L-1)} Y_{L-1, m-m'}^*(\vartheta_Q, \varphi_Q) \\ &\times GC(1, L, L-1, m, m') \int r^2 dr \\ &\times R_{n1}(r)^* R_{n' L}(r) j_{L-1}(Qr) \\ &+ i^{(L+1)} Y_{L+1, m-m'}^*(\vartheta_Q, \varphi_Q) \\ &\times GC(1, L, L+1, m, m') \int r^2 dr \\ &\times R_{n1}(r)^* R_{n' L}(r) j_{L+1}(Qr). \end{aligned} \quad (12)$$

since $GC(1, L, L, m, m') = 0$. The factors $GC(l, l', l'', m, m')$ are defined as

$$GC(l, l', l'', m, m') = \langle Y_{lm} | Y_{l'' m''-m} | Y_{l' m'} \rangle. \quad (13)$$

We note that all terms in the l -expansion have the same m'' . But as the total overlap between the $|P8, X\Gamma_4^- \rangle$ and all the other states consists of contributions with different m'' , we cannot take out from W a common factor $\exp(im''\varphi_Q)$, so the overlap integrals also depend on the azimuth φ_Q . As example we write down the overlap integral between $|P8, X\Gamma_4^- \rangle$ and the states

derived from the Γ_3^+ envelope functions

$$\begin{aligned} \langle P, X | e^{i\vec{Q} \cdot \vec{r}} | D3, XY \rangle &= i4\pi [CG(1211, 0) \text{Re}(Y_{11}(\vartheta_Q, \varphi_Q)) W_R(n1n'2, 1) \\ &+ \text{Re}(Y_{3-1}(\vartheta_Q, \varphi_Q)) CG(12310)) W_R(n1n'2, 3)] \\ \langle P, X | e^{i\vec{Q} \cdot \vec{r}} | D3, XZ \rangle &= \frac{4\pi}{\sqrt{8}} [Y_{10}(\vartheta_Q, \varphi_Q) \\ &\times CG(12100) W_R(n1n'2, 1) + (Y_{30}(\vartheta_Q, \varphi_Q) CG(12300) \\ &- \sqrt{\frac{3}{2}} \text{Re}(Y_{32}(\vartheta_Q, \varphi_Q)) CG(12302)) W_R(n1n'2, 3)] \\ \langle P, X | e^{i\vec{Q} \cdot \vec{r}} | D3, YZ \rangle &= 0 \\ \langle P, X | e^{i\vec{Q} \cdot \vec{r}} | D3, X \rangle &= 0 \\ \langle P, X | e^{i\vec{Q} \cdot \vec{r}} | D3, Y \rangle &= -\frac{1}{2} 4\pi [(CG(12302) \\ &\times \text{Re}(Y_{32}(\vartheta_Q, \varphi_Q)) + \sqrt{\frac{3}{2}} Y_{30}(\vartheta_Q, \varphi_Q) CG(12300)) \\ &\times W_R(n1n'2, 3) \\ &+ \sqrt{\frac{3}{2}} \{Y_{10}(\vartheta_Q, \varphi_Q) CG(12100) W_R(n1n'2, 1)\}] \\ \langle P, X | e^{i\vec{Q} \cdot \vec{r}} | D3, Z \rangle &= -\frac{i}{\sqrt{2}} 4\pi [CG(12112) \\ &\times \text{Re}(Y_{11}(\vartheta_Q, \varphi_Q)) W_R(n1n'2, 1) \\ &+ (CG(1231-2) \text{Re}(Y_{33}(\vartheta_Q, \varphi_Q)) + CG(12312) \\ &\times \text{Re}(Y_{31}(\vartheta_Q, \varphi_Q))) W_R(n1n'2, 3)]. \end{aligned} \quad (14)$$

So in calculating the scattering rates we have to integrate also over the angle φ .

3. Plasmons and coupling with LO phonons

Assuming a plasma with density ρ_{eh} and temperature T we have the plasma frequency [6]

$$\omega_{\text{pl}}^2 = \frac{e_0^2}{\varepsilon_0 \varepsilon_{\text{st}} \mu_{\text{eh}}} \rho_{\text{eh}}, \quad (15)$$

where ε_{st} is the static dielectric constant of the crystal and $\mu_{\text{eh}} = (1/m_{\text{e}}^* + 1/m_{\text{h}}^*)^{-1}$ the reduced electron–hole mass with individual masses m_{e}^* and m_{h}^* .

The plasmon dispersion $\omega_{\text{p}}(q)$ is determined by the zeros of the real part of the dielectric function (DF) $\varepsilon(q, \omega)$ [6]

$$\text{Re}(\varepsilon(q, \omega_{\text{p}}(q))) = 0, \quad (16)$$

while the damping is given by

$$\gamma(q) = \frac{\text{Im}(\varepsilon(q, \omega + i\delta))}{\frac{\partial}{\partial \omega} \text{Re}(\varepsilon(q, \omega))} \Big|_{\omega=\omega_p(q)} \quad (17)$$

The detailed form of the DF depends on the composition of the plasma and the degree of degeneracy which is given by the product of density and thermal de Broglie wavelength [6]. In case of an electron–hole plasma with temperature T_{eh} this product is given as

$$\rho_{\text{eh}} \left(\frac{2\pi\hbar^2}{\mu_{\text{eh}}k_B T_{\text{eh}}} \right)^{3/2} \quad (18)$$

For the relevant densities below 10^{12} cm^{-3} and temperatures above 1 K this product is much smaller than 1 so that we are always in the non-degenerate regime. Here the plasmon properties have been investigated thoroughly (see e.g. [6]).

The plasma dispersion is given by

$$\omega_p^2(q) = \omega_{\text{pl}}^2 \left(1 + \frac{3q^2}{\kappa_{\text{nd}}^2} \right), \quad (19)$$

with the screening vector

$$\begin{aligned} \kappa_{\text{nd}}^2 &= \frac{\omega_{\text{pl}}^4}{\sum_i \rho_i e_i^2 k_B T / (\varepsilon_{\text{st}} \varepsilon_0 m_i^2)} = \kappa_{\text{D}}^2 \cdot \left(\frac{1}{2} \frac{(m_c + m_v)^2}{m_c^2 + m_v^2} \right) \\ &= 0.965^2 \kappa_{\text{D}}^2, \end{aligned} \quad (20)$$

where κ_{D} is the Debye wave number [6].

The numerical value applies for Cu_2O .

The plasmon damping can be derived from (17), but we will use a simplified consideration according to which a well-defined plasmon exists only outside the single-particle excitation regime, i.e., for wave vectors

$$q < q_{\text{max}} = \kappa_c \left(\sqrt{1 + \frac{2\omega_p(q)}{\omega_c}} - 1 \right) \quad \text{with } \omega_c = \frac{\hbar\kappa_c^2}{\mu_{\text{eh}}}, \quad (21)$$

where κ_c is a critical wave number that for $T = 0$ can be taken as the Fermi wave number $\kappa_{\text{F}} = (3\pi^2\rho_{\text{eh}})^{1/3}$.

Note that this already rules out any scattering from the nP states to the $1S$ state, as the wave vector required is much larger than allowed by (21).

However, these considerations neglect that in polar crystals the plasmons are coupled to the LO phonons giving rise to a coupled phonon-plasmon mode (see e.g. [8]). If Ω_{LO} denotes the LO frequency, we have the relation

$$\Omega_{\text{TO}} = \sqrt{\frac{\varepsilon_{\text{inf}}}{\varepsilon_{\text{st}}}} \Omega_{\text{LO}}. \quad (22)$$

The coupled modes are obtained from the solution of the dispersion relation

$$\omega^4 - \omega^2(\Omega_{\text{LO}}^2 + \omega_{\text{pl}}^2 + \omega_q^2) + \Omega_{\text{TO}}^2(\omega_{\text{pl}}^2 + \omega_q^2) = 0, \quad (23)$$

with the plasma frequency ω_{pl} and

$$\omega_q^2 = \frac{3q^2}{\kappa_{\text{nd}}^2} \omega_{\text{pl}}^2. \quad (24)$$

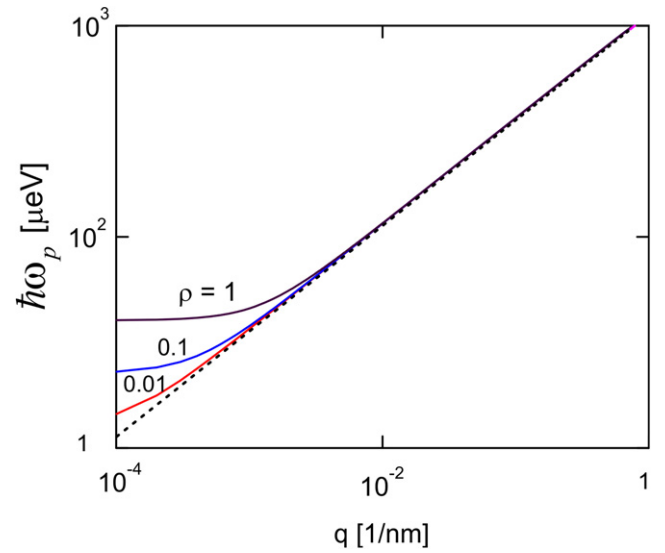


Figure 1. Coupled phonon-plasmon dispersions in Cu_2O for different densities as indicated (in units of μm^{-3}) and a temperature of 12 K. The dotted line gives the linear approximation.

Note that this expression differs from that used in [8] where it is $\omega_p(q) = \langle v^2 \rangle q^2 / 3\varepsilon_{\infty}$ (ε_{∞} denotes the dielectric constant for infinite frequency) and $\langle v^2 \rangle = 3k_B T / m^*$ is the average squared velocity of the non-degenerate electron gas.

The solutions of (23) are given as

$$\begin{aligned} \omega_{\pm}^2(q) &= \frac{1}{2} (\Omega_{\text{LO}}^2 + \omega_{\text{pl}}^2 + \omega_q^2) \\ &\pm \sqrt{\frac{1}{4} (\Omega_{\text{LO}}^2 + \omega_{\text{pl}}^2 + \omega_q^2)^2 - \Omega_{\text{TO}}^2 (\omega_{\text{pl}}^2 + \omega_q^2)}. \end{aligned} \quad (25)$$

A typical example of a dispersion relation for the lower mode is shown in figure 1 for different plasma densities and a temperature of 12 K. One sees that the dispersion, especially for low plasma densities is almost linear. Therefore we can describe the plasma dispersion by a sound velocity which is density independent, but depends on the plasma temperature as $u_{\text{pl}}(T) = 5.76 \times 10^3 \text{ m s}^{-1} \sqrt{T \text{ K}^{-1}}$ (acoustic model). This approximation is valid in the range of wave numbers of interest (see figure 2) and simplifies the calculations below considerably.

The scattering efficiency of a coupled mode can be calculated from the effective charge of the mode in close analogy to the pure phonon (see [8]). For a Fröhlich-type interaction of polar optical phonons it is given as

$$\Xi_{\text{c,v}}^{\text{LO}}(Q) = \sqrt{\frac{\hbar\omega_{\text{LO}}e_0^2}{2\varepsilon_0 N \Omega_0}} \sqrt{\frac{1}{\varepsilon^*}} \cdot \frac{1}{Q} = \sqrt{\frac{e_0 e_{\text{LO}}^*}{2M_{\text{ion}} \varepsilon_0 N \Omega_0 \Omega_{\text{LO}}}} \frac{1}{Q}. \quad (26)$$

Here $\hbar\omega_{\text{LO}}$ denotes the phonon energy, ε^* denotes the effective dielectric constant of the phonon mode given as

$$\frac{1}{\varepsilon^*} = \frac{1}{\varepsilon_{\text{up}}} - \frac{1}{\varepsilon_{\text{low}}}, \quad (27)$$

where $\varepsilon_i^{\text{up,low}}$ denotes the dielectric constant above and below the phonon mode.

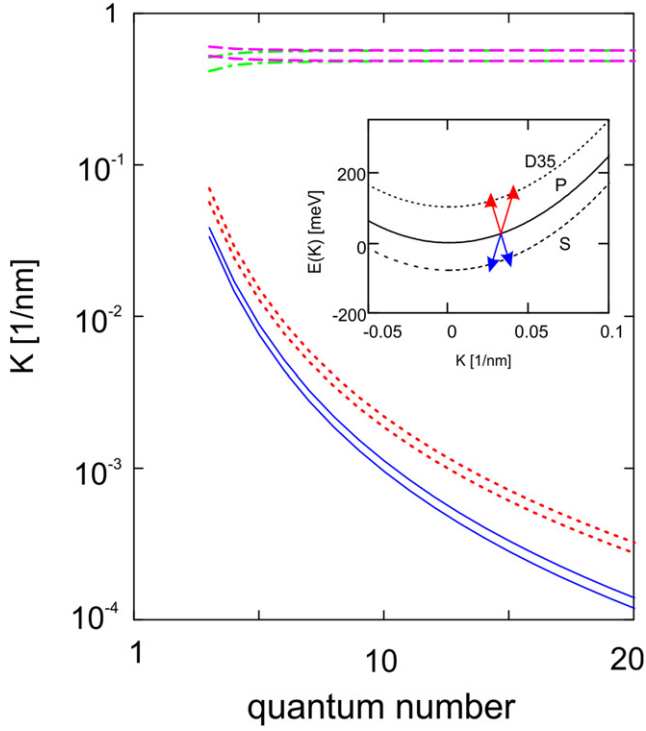


Figure 2. Limits for the Q integration in as function of main quantum number n for $nP \rightarrow nS$ and $nP \rightarrow nD35$ processes. The blue full lines gives the limits for the Stokes process in case of $nP \rightarrow nS$ (as indicated by the blue arrows in the inset), the red dotted lines give the limits of the anti-Stokes process in case of $nP \rightarrow nD35$ (red arrows in the inset). The green dot-dashed and the magenta dot-dashed lines give the limits for the anti-Stokes $nP \rightarrow nS$ and the second anti-Stokes process for $nP \rightarrow nD35$.

The effective charge of the LO mode is given by

$$e_{\text{LO}}^* = \sqrt{M_{\text{ion}} N \Omega_0 \varepsilon_0 \left(\frac{1}{\varepsilon_{\infty}} - \frac{1}{\varepsilon_{\text{st}}} \right)} \Omega_{\text{LO}}. \quad (28)$$

The matrix element of the coupled plasmon-phonon scattering of an electron with wave vector q is [8]

$$M = \left[\frac{e_0 e^*}{M_{\text{ion}} N \Omega_0 \varepsilon_0 \omega_{-}(q) q^2} \right]^{1/2}, \quad (29)$$

with the effective charge

$$e^* = e_{\text{LO}}^* \cdot R. \quad (30)$$

With a function R given by

$$R = \left(\frac{\omega_{\pm}^2 - \Omega_{\text{TO}}^2}{\Omega_{\text{LO}}^2 - \Omega_{\text{TO}}^2} \right) \cdot \left[1 + \frac{(\omega_{\text{pl}}^2 + \omega_q^2)^2 (\omega_{\pm}^2 - \Omega_{\text{TO}}^2)^2}{\omega_{\text{pl}}^4 (\Omega_{\text{LO}}^2 - \Omega_{\text{TO}}^2)} \right]^{-1/2}, \quad (31)$$

this gives finally for M

$$M = \left[\frac{e_0^2 \Omega_{\text{LO}}^2}{2 \varepsilon_0 \omega_{-}(q) q^2} \left(\frac{1}{\varepsilon_{\infty}} - \frac{1}{\varepsilon_{\text{st}}} \right) \right]^{1/2} \cdot R. \quad (32)$$

As electron and hole masses we use polaron masses $m_e^* = 0.985 m_e$ $m_h^* = 0.575 m_e$ [16], which gives as exciton

mass for the states with $n \geq 2$ $M_X = 1.56 m_e$ and a reduced mass $\mu_{\text{eh}} = 0.356 m_e$. In Cu_2O we have the complication that there are two LO modes with phonon energies (see e.g. [17])

$$\begin{aligned} E_{\text{TO}1} &= 18.8 \text{ meV} & E_{\text{LO}1} &= 19.1 \text{ meV} \\ E_{\text{TO}2} &= 78.5 \text{ meV} & E_{\text{LO}2} &= 82.1 \text{ meV}, \end{aligned} \quad (33)$$

and effective ε_i^* ($\varepsilon_1^* = 233$, $\varepsilon_2^* = 76$) corresponding to $\varepsilon_{\text{st}} = 7.53$ and $\varepsilon_{\infty} = 6.47$. To be able to use the theory developed above, we consider instead an effective phonon with energy $E_{\text{LO}} = \sqrt{E_{\text{LO}1} E_{\text{LO}2}}$ and $E_{\text{TO}} = \sqrt{\varepsilon_{\infty} / \varepsilon_{\text{st}}} E_{\text{LO}}$.

The scattering rate by plasmons between the initial exciton state $|nlm; \vec{K}\rangle$ and a specified final state $|n'l'm'\rangle$ is given by

$$\begin{aligned} \Gamma(nlm, \vec{K}; n'l'm') &= \frac{2\pi N \Omega_0}{\hbar 8\pi^3} \int_0^{\infty} dQ Q^2 \\ &\times \left(n_B(\hbar\omega_{\text{pl}}(Q, T)) + \frac{1}{2} \pm \frac{1}{2} \right) \\ &\times \int_0^{\pi} \int_0^{2\pi} d\varphi \left| M(\vec{K}, nlm, \vec{K} \right. \\ &\left. \pm \vec{Q}, n'l'm', Q, \vartheta, \varphi) \right|^2 \delta(E_i - E_f) \sin \vartheta d\vartheta. \end{aligned} \quad (34)$$

Here, one has to distinguish between (i) Stokes (phonon emission, upper sign) and (ii) anti-Stokes (phonon absorption, lower sign) processes. $n_B(\hbar\omega, T)$ is the Bose distribution. We have

$$\begin{aligned} \text{(i)} \quad E_i &= E_g - E_{\text{BX}}(n, l) + \frac{\hbar^2 \vec{K}^2}{2M_{Xn}}, \\ E_f &= E_g - E_{\text{BX}}(n', l') + \frac{\hbar^2 (\vec{K} + \vec{Q})^2}{2M_{Xn'}} + \hbar\omega_{\text{pl}}(\vec{Q}), \\ \text{(ii)} \quad E_i &= E_g - E_{\text{BX}}(n, l) + \frac{\hbar^2 \vec{K}^2}{2M_{Xn}} + \hbar\omega_{\text{pl}}(\vec{Q}), \\ E_f &= E_g - E_{\text{BX}}(n', l') + \frac{\hbar^2 (\vec{K} - \vec{Q})^2}{2M_{Xn'}}. \end{aligned} \quad (35)$$

where $E_{\text{BX}}(n, l)$ is the binding energy of the state with quantum numbers n, l . We see, that the argument of the delta-function depends on the angle ϑ between \vec{K} and \vec{Q} and on the magnitude of \vec{Q} . Note that the excitons are excited at the finite optical wave vector $K_{\text{opt}} = n_b(E_g - Ry/n^2)/\hbar c_0$ [17]. In calculating (34) we follow closely the procedure in [17], note that we have here $\kappa = M_X u_{\text{pl}}/\hbar$, thereby assuming that $\omega_{\text{pl}}(Q) = u_{\text{pl}} Q$.

4. Calculation of the scattering rates

For this we have to take the fine structure of the Rydberg excitons into account (see section 1). Since $nP \rightarrow nP$ Stokes scattering is not possible because $\kappa > K_{\text{opt}}$, we have to consider $nP \rightarrow nS$ and $nP \rightarrow nD$ scattering. From the conditions

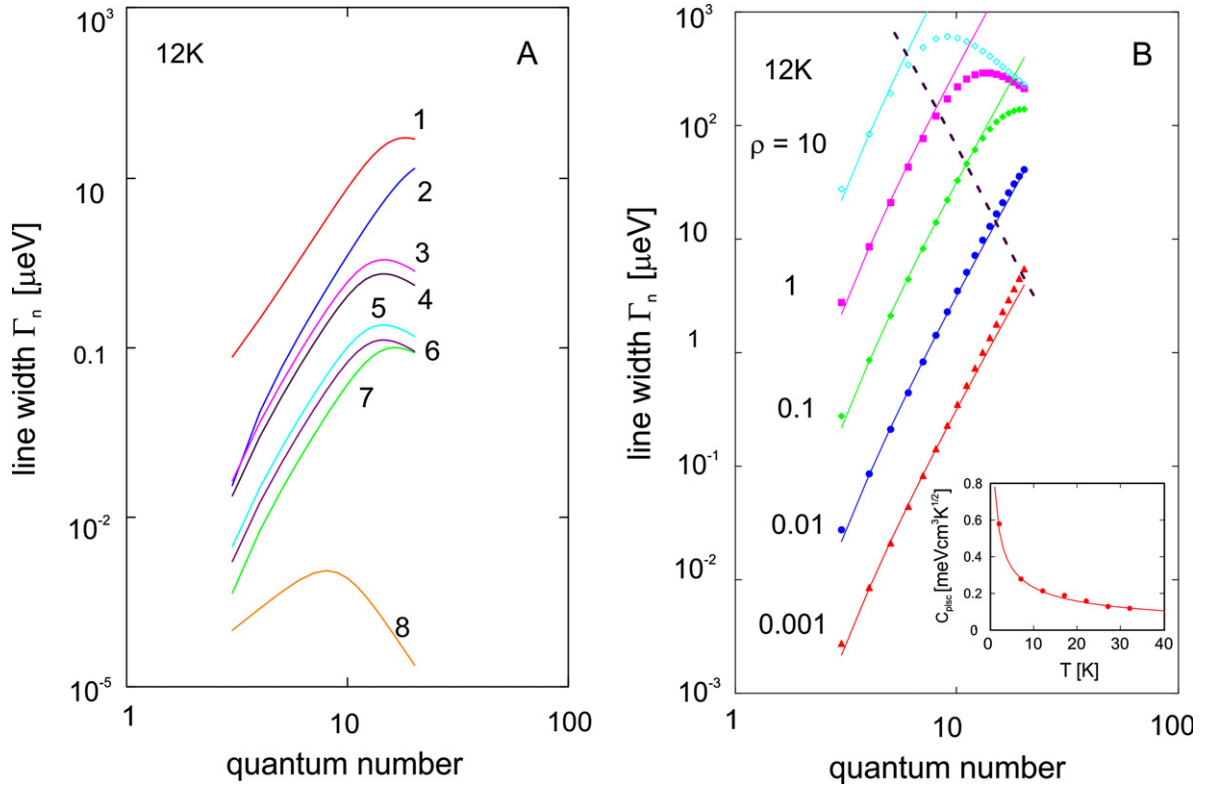


Figure 3. Line broadening due to exciton-plasmon scattering as function of quantum number n of the P exciton state. The left diagram (A) shows the relaxation rates for some possible scattering processes for an electron–hole density of $\rho_{\text{eh}} = 0.1 \mu\text{m}^{-3}$ and a plasma temperature of $T_{\text{eh}} = 12$ K as indicated (1 = $nP \rightarrow nS$, 2 = $nP \rightarrow nD35$, 3 = $nP \rightarrow nD564$, 4 = $nP \rightarrow nD34$, 5 = $nP \rightarrow n585$, 6 = $nP \rightarrow nD561$, 7 = $nP \rightarrow nD584$ and 8 = $nP \rightarrow nP$). The right diagram (B) shows the sum of all processes for different densities as indicated (in units of μm^{-3}) and $T_{\text{eh}} = 12$ K. The full lines give the scaling law. The dashed line indicates the Mott point for the corresponding quantum number at which the exciton state vanishes [6]. The inset in part (B) shows the temperature dependence of the proportionality constant of.

of energy and momentum conservation one can easily derive that scattering into the lower lying S states is possible both by Stokes (type 1) and anti-Stokes processes (type 2) while the higher energy D states can only be reached by anti-Stokes scattering (type 2). The integration limits depend strongly on the quantum number and are depicted for the different processes in figure 2. Here we see that for $nP \rightarrow nS$ the wave numbers for the anti-Stokes process (green dot-dashed lines) are very large, so that the occupation number of these plasmons is very small and can be neglected. For $nP \rightarrow nD$ (here the case of the $D355$ states) there are two regions where anti-Stokes scattering is possible, but only the processes marked by red dotted lines have sufficient occupation. The maximum possible plasmon wave number q_{max} (see (21)) is here about 0.23 nm^{-1} .

The results of the integrations are shown in figure 3(A) for typical densities ($\rho_{\text{eh}} = 10^{11} \text{ cm}^{-3}$) and temperatures ($T_{\text{eh}} = 17$ K) of an electron–hole plasma present in optically pumped Cu_2O [3].

The two dominant processes are the scattering into the $S\Gamma_5^+$ and the $D3\Gamma_5^+$ exciton states (red and blue lines in figure 3(A)). The sum of the rates nicely follows a power law for quantum numbers up to $n = 12$

$$\Gamma_{\text{pl}}(n, T) = C_{\text{plsc}}(T)\rho_{\text{eh}}(n-1)^{3.3}, \quad (36)$$

with a proportionality factor $C_{\text{plsc}}(12 \text{ K}) = 0.235 \mu\text{eV} \mu\text{m}^3$. As shown in the inset of figure 3(B), the proportionality factor

strongly depends on temperature following closely a relation (for details see appendix B)

$$C_{\text{plsc}}(T) = 0.8/\sqrt{T} \mu\text{eV} \mu\text{m}^3 \text{K}^{1/2}. \quad (37)$$

To give an order of magnitude of the effect, we calculate the broadening for a typical plasma density of $\rho_{\text{eh}} = 10^{11} \text{ cm}^{-3}$ and a temperature of $T_{\text{eh}} = 15$ K. For $n = 10$ we obtain a broadening of $32 \mu\text{eV}$ which should be easily detectable experimentally [3].

In conclusion, we have demonstrated that Rydberg excitons in Cu_2O which are embedded in a low-density electron–hole plasma undergo strong scattering between different angular momentum states (S , P and D) that are energetically split due to the non-parabolicity of the band structure. Since in all experiments performed up to now involving Rydberg excitons, the creation of a low-density plasma is unavoidable due to congruent excitation of yellow $1S$ exciton states by the indirect phonon-assisted background absorption and subsequent Auger-like decay processes of these excitons [18–21], we expect that the plasmon induced broadening is of high significance and must be taken into account in the interpretation.

Furthermore, we expect that this scattering mechanism is also important in other semiconductors which show a splitting of exciton states with different angular momentum due

to a non-parabolicity of the valence or conduction bands, like III–V and II–VI materials [7] and also in two-dimensional semiconductor structures as WSe₂ [22].

Acknowledgments

We thank Wolf-Dietrich Kraeft and Peter Grünwald for clarifying discussions. DS thanks the Deutsche Forschungsgemeinschaft for financial support (Project Number SE 2885/1-1).

Data availability statement

The data that support the findings of this study are available upon reasonable request from the authors.

Appendix A. Symmetry decomposition of S, P and D exciton states

S states

$$\begin{aligned} |S, \Gamma_2^+\rangle &= SP \\ |S, XY\Gamma_5^+\rangle &= SO_{xy} \\ |S, XZ\Gamma_5^+\rangle &= SO_{xz} \\ |S, YZ\Gamma_5^+\rangle &= SO_{yz}. \end{aligned} \quad (\text{A1})$$

P states

$$\begin{aligned} |P7, \Gamma_2^-\rangle &= -\frac{1}{\sqrt{3}}P_xO_{yz} + \frac{1}{\sqrt{3}}P_yO_{xz} + \frac{1}{\sqrt{3}}P_zO_{xy} \\ |P7, YZ\Gamma_5^-\rangle &= -\frac{1}{\sqrt{3}}P_xP - \frac{1}{\sqrt{3}}P_yO_{xy} + \frac{1}{\sqrt{3}}P_zO_{xz} \\ |P7, XZ\Gamma_5^-\rangle &= \frac{1}{\sqrt{3}}P_xO_{xy} - \frac{1}{\sqrt{3}}P_yP - \frac{1}{\sqrt{3}}P_zO_{yz} \\ |P7, XY\Gamma_5^-\rangle &= -\frac{1}{\sqrt{3}}P_xO_{xz} + \frac{1}{\sqrt{3}}P_yO_{yz} - \frac{1}{\sqrt{3}}P_zP \\ |P8, 1\Gamma_3^-\rangle &= -\frac{1}{\sqrt{2}}P_yO_{xy} - \frac{1}{\sqrt{2}}P_zO_{xz} \\ |P8, 2\Gamma_3^-\rangle &= -\frac{1}{\sqrt{2}}P_xO_{xy} - \frac{1}{\sqrt{2}}P_zO_{yz} \\ |P8, X\Gamma_4^-\rangle &= -\frac{1}{\sqrt{2}}P_yO_{xy} - \frac{1}{\sqrt{2}}P_zO_{xz} \\ |P8, Y\Gamma_4^-\rangle &= -\frac{1}{\sqrt{2}}P_xO_{xy} - \frac{1}{\sqrt{2}}P_zO_{yz} \\ |P8, Z\Gamma_4^-\rangle &= -\frac{1}{\sqrt{2}}P_xO_{xz} - \frac{1}{\sqrt{2}}P_yO_{yz} \\ |P8, YZ\Gamma_5^-\rangle &= -\frac{1}{\sqrt{2}}P_yO_{xy} - \frac{1}{\sqrt{2}}P_zO_{xz} \\ |P8, XZ\Gamma_5^-\rangle &= -\frac{1}{\sqrt{2}}P_xO_{xy} - \frac{1}{\sqrt{2}}P_zO_{yz} \\ |P8, YZ\Gamma_5^-\rangle &= -\frac{1}{\sqrt{2}}P_xO_{xz} - \frac{1}{\sqrt{2}}P_yO_{yz}. \end{aligned} \quad (\text{A2})$$

D states

D3 derived

$$\begin{aligned} |D3, 1\Gamma_3^+\rangle &= |d_{x^2-y^2}\rangle P \\ |D3, 2\Gamma_3^+\rangle &= |d_{z^2}\rangle P \\ |D3, XY\Gamma_5^+\rangle &= -|d_{z^2}\rangle O_{xy} \\ |D3, YZ\Gamma_5^+\rangle &= \frac{1}{2}(|d_{z^2}\rangle + \sqrt{3}|d_{x^2-y^2}\rangle)O_{yz} \\ |D3, XZ\Gamma_5^+\rangle &= \frac{1}{2}(|d_{z^2}\rangle - \sqrt{3}|d_{x^2-y^2}\rangle)O_{xz} \\ |D3, Z\Gamma_4^+\rangle &= -|d_{x^2-y^2}\rangle O_{xy} \\ |D3, X\Gamma_4^+\rangle &= \frac{1}{2}(|d_{x^2-y^2}\rangle - \sqrt{3}|d_{z^2}\rangle)O_{yz} \\ |D3, Y\Gamma_4^+\rangle &= \frac{1}{2}(|d_{x^2-y^2}\rangle + \sqrt{3}|d_{z^2}\rangle)O_{xz}. \end{aligned} \quad (\text{A3})$$

D5 derived

$$\begin{aligned} |D5, 6, \Gamma_1^+\rangle &= \frac{1}{\sqrt{3}}d_{yz}O_{yz} + \frac{1}{\sqrt{3}}d_{xz}O_{xz} + \frac{1}{\sqrt{3}}d_{xy}O_{xy} \\ |D5, 6, X\Gamma_4^+\rangle &= -\frac{1}{\sqrt{3}}d_{yz}P + \frac{1}{\sqrt{3}}d_{xz}O_{xy} + \frac{1}{\sqrt{3}}d_{xy}O_{xz} \\ |D5, 6, Y\Gamma_4^+\rangle &= \frac{1}{\sqrt{3}}d_{yz}O_{xy} - \frac{1}{\sqrt{3}}d_{xz}P - \frac{1}{\sqrt{3}}d_{xy}O_{yz} \\ |D5, 6, Z\Gamma_4^+\rangle &= -\frac{1}{\sqrt{3}}d_{yz}O_{xz} - \frac{1}{\sqrt{3}}d_{xy}P + \frac{1}{\sqrt{3}}d_{xz}O_{yz} \\ |D5, 8, 1\Gamma_3^+\rangle &= -\frac{1}{\sqrt{2}}P_yO_{xy} - \frac{1}{\sqrt{2}}P_zO_{xz} \\ |D5, 8, 2\Gamma_3^+\rangle &= -\frac{1}{\sqrt{2}}P_xO_{xy} - \frac{1}{\sqrt{2}}P_zO_{yz} \\ |D5, 8, X\Gamma_4^+\rangle &= +\frac{1}{\sqrt{6}}d_{yz}P + \frac{1}{\sqrt{6}}d_{xy}O_{xz} - \frac{1}{\sqrt{6}}d_{xz}O_{xy} \\ |D5, 8, Y\Gamma_4^+\rangle &= -\frac{1}{\sqrt{6}}d_{yz}O_{xy} + \frac{2}{\sqrt{6}}d_{xz}P - \frac{1}{\sqrt{6}}d_{xy}O_{yz} \\ |D5, 8, Z\Gamma_4^+\rangle &= -\frac{1}{\sqrt{6}}d_{yz}O_{xz} + \frac{1}{\sqrt{6}}d_{xz}O_{yz} + \frac{2}{\sqrt{6}}d_{xy}P \\ |D5, 8, YZ\Gamma_5^+\rangle &= \frac{1}{\sqrt{2}}d_{xy}O_{xz} + \frac{1}{\sqrt{2}}d_{xz}O_{xy} \\ |D5, 8, XZ\Gamma_5^+\rangle &= \frac{1}{\sqrt{2}}d_{yz}O_{xy} + \frac{1}{\sqrt{2}}d_{xy}O_{yz} \\ |D5, 8, XY\Gamma_5^+\rangle &= \frac{1}{\sqrt{2}}d_{yz}O_{xz} + \frac{1}{\sqrt{2}}d_{xz}O_{yz}. \end{aligned} \quad (\text{A4})$$

Appendix B. Scattering rates of all processes for different densities and temperatures

Here we give all scattering rates for a density range from 10^9 cm^{-3} to 10^{13} cm^{-3} (indicated in the figures in units of μm^{-3}) and temperatures $T_{\text{eh}} = 2 \text{ K}$ to $T_{\text{eh}} = 32 \text{ K}$ and principal quantum numbers from 3 to 20; for $T_{\text{eh}} = 12 \text{ K}$ see figure 3).

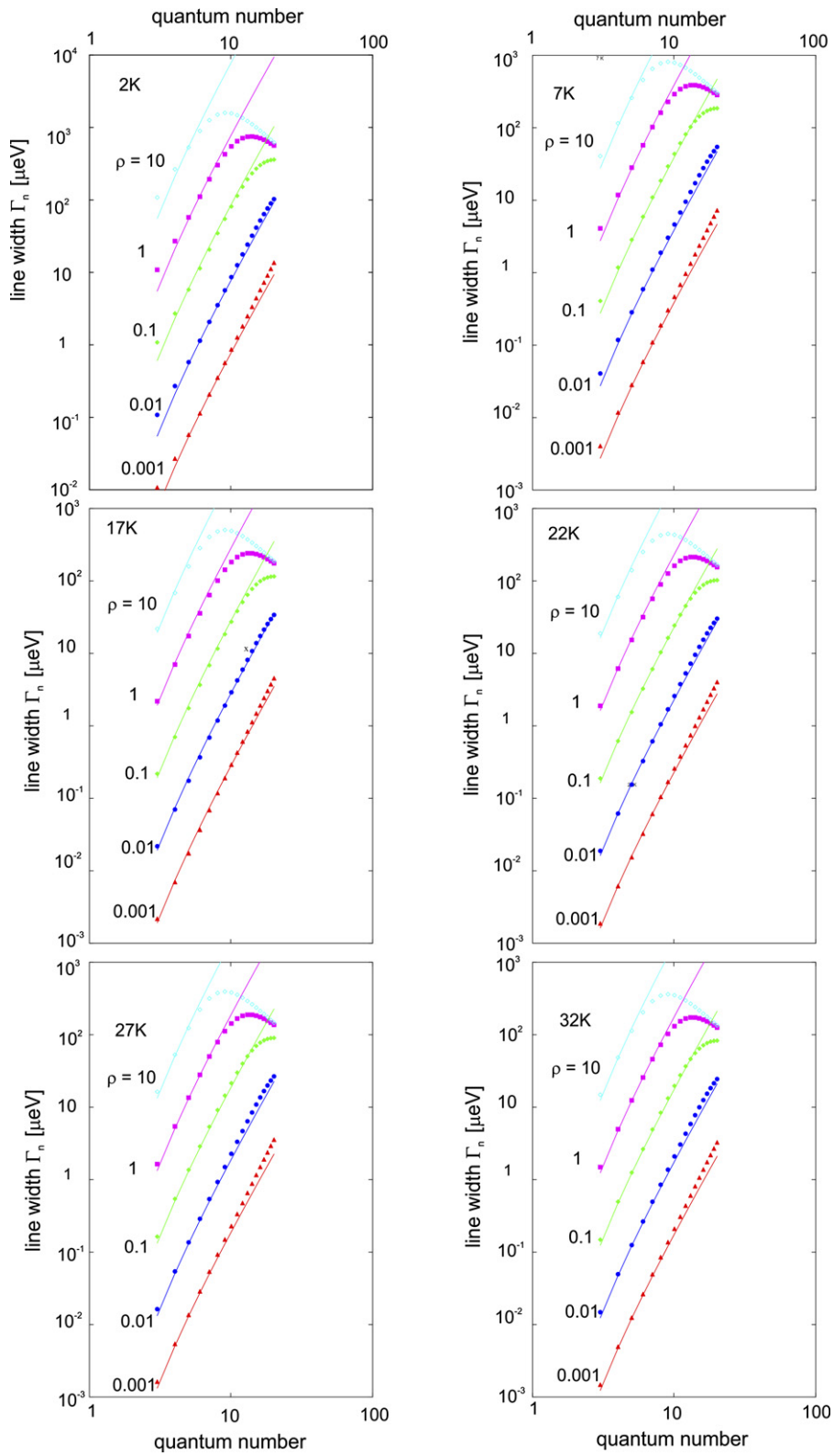


Figure 4. Total scattering rates for different densities and temperatures. The full lines give the scaling law.

ORCID iDsHeinrich Stolz  <https://orcid.org/0000-0002-2678-3854>Dirk Semkat  <https://orcid.org/0000-0002-2179-9064>**References**

- [1] Kazimierczuk T, Fröhlich D, Scheel S, Stolz H and Bayer M 2014 *Nature* **514** 343
- [2] Aßmann M and Bayer M 2020 *Adv. Quantum Technol.* **3** 1900134
- [3] Heckötter J *et al* 2018 *Phys. Rev. Lett.* **121** 097401
- [4] Semkat D, Fehske H and Stolz H 2019 *Phys. Rev. B* **100** 155204
- [5] Semkat D, Fehske H and Stolz H 2021 *Eur. Phys. J. Spec. Top.* **230** 947
- [6] Kremp D, Schlanges M and Kraeft W D 2005 *Quantum Statistics of Nonideal Plasmas* (Berlin: Springer)
- [7] Klingshirn C 2012 *Semiconductor Optics* 4th edn (New York: Springer)
- [8] Ridley B K 2013 *Quantum Processes in Semiconductors* 5th edn (Oxford: Oxford University Press)
- [9] Schöne F *et al* 2016 *Phys. Rev. B* **93** 075203
- [10] Schöne F *et al* 2016 *J. Phys. B: At. Mol. Opt. Phys.* **49** 134003
- [11] Heckötter J, Freitag M, Fröhlich D, Aßmann M, Bayer M, Semina M A and Glazov M M 2017 *Phys. Rev. B* **95** 035210
- [12] Schweiner F, Main J, Wunner G and Uihlein C 2017 *Phys. Rev. B* **95** 195201
- [13] Toyozawa Y 1958 *Prog. Theor. Phys.* **20** 53
- [14] Koster G F 1963 *Properties of the Thirty-Two Point Groups* (Cambridge, MA: MIT Press)
- [15] Heckötter J 2020 *Thesis* TU Dortmund
- [16] Naka N, Akimoto I, Shirai M and Kan'no K 2012 *Phys. Rev. B* **85** 035209
- [17] Stolz H, Schöne F and Semkat D 2018 *New J. Phys.* **20** 023019
- [18] Kavoulakis G M and Baym G 1996 *Phys. Rev. B* **54** 16625
- [19] O'Hara K E, Gullingsrud J R and Wolfe J P 1999 *Phys. Rev. B* **60** 10872
- [20] Yoshioka K, Idegushi T, Mysyrowicz A and Kuwata-Gonokami M 2010 *Phys. Rev. B* **82** 041202
- [21] Semkat D, Sobkowiak S, Schöne F, Stolz H, Koch T and Fehske H 2017 *J. Phys. B: At. Mol. Opt. Phys.* **50** 204001
- [22] Respondek P 2021 private communication